Plane Wave Scattering by Slots on a Ground Plane Loaded with Semicircular Dielectric Cylinders in Case of Oblique Incidence and Arbitrary Polarization

Ioannis O. Vardiambasis, John L. Tsalamengas, *Member, IEEE*, and John G. Fikioris

***Abstract*— Plane wave scattering by single or double slots loaded with semicircular dielectric cylinders is investigated in the most general case of oblique incidence and arbitrary polarization. To this end, systems of singular integral-integrodifferential equations of the first kind are constructed and discretized on the basis of recently developed algorithms. Several internal tests and extensive comparisons with available results were made in order to validate the numerical codes. Plotted results both for the surface magnetic current densities and the radar cross sections reveal how the scattering properties may be controlled by changing several physical and geometrical parameters of the structure.**

I. Introduction

DIELECTRIC loads are often used as convenient means for modifying the scattering properties of the basic slot scatterer. In particular, radar cross-section reduction and control can be achieved by proper selection of certain geometrical and physical parameters like dielectric constants, slot dimensions, and angle of incidence. In addition, dielectrically loaded slots in the form of finlines and microslot-lines are widely used in microwave and millimeter-wave integrated circuit (MMIC) technology for reasons of easy fabrication and conformability.

In this paper, we investigate scattering of arbitrarily polarized plane waves obliquely incident on a two-dimensional slot (or a couple of such slots) in the presence of semicylindrical dielectric loads (in general lossy). Figs. 1 and 2 show two basic configurations from which a number of interesting structures may be derived as special cases, some of which are shown in Fig. 3.

The analysis is based on systems of singular integral-integrodifferential equations (SIE-SIDE) of the first kind with unknowns the equivalent surface magnetic current densities across the slot(s). These systems are discretized using recently developed algorithms, which lead to efficient analytical expressions for the matrix elements. Analytical expressions are also derived for the scattered field.

Previous papers [1]–[8]are concerned with the special (and simpler) case of normal incidence, where TE and TM (to slot axis) waves decouple and can be treated separately. Reference [1] deals with the structures of Fig. 3(a)–(b), while [2]–[6] [dealing with the structure of Fig. 3(c)] and [7] [dealing with the structure of Fig. 3(d)] are further restricted to the case $\varepsilon_1 = \varepsilon_2, w = a$.

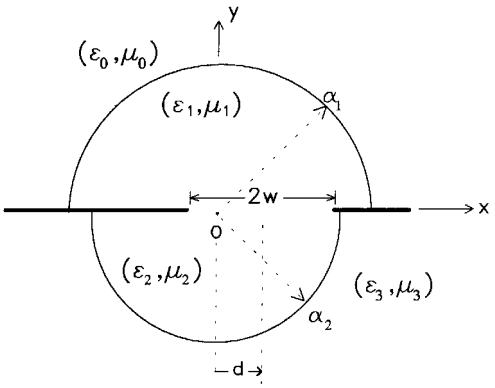

(a)

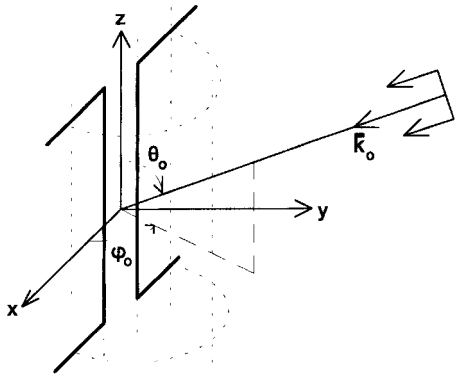

(b)

Fig. 1. (a) Geometry of a slot loaded with two semicylinders. (b) The incident plane wave.

Extensive comparisons with the results of [2]–[8] (for $w = a$) and of [1] have been carried out to test the numerical codes and, in addition, several internal tests based on energy conservation principles were applied. The agreement in all cases was excellent.

We further note that the novel microslotlines shown in Fig. 3(a)–(d) can be treated on the basis of a system of SIE-SIDE's, which, apart from being homogeneous, is identical with the system of equations used for the scattering problem in this paper. The aforementioned tests are, therefore, useful in validating the numerical codes for these propagation problems

Manuscript received March 31, 1995; revised March 15, 1998.

The authors are with the Department of Electrical and Computer Engineering, National Technical University of Athens, Zografou GR-15773, Athens, Greece.

Publisher Item Identifier S 0018-926X(98)06107-9.

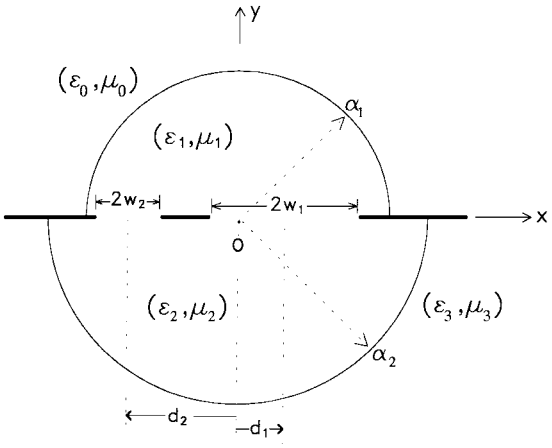

Fig. 2. Geometry of two coplanar slots on an infinite perfectly conducting planar interface between two semicylindrical loads. The centers of the slots are at $x = d_1$ and $x = -d_2$, respectively.

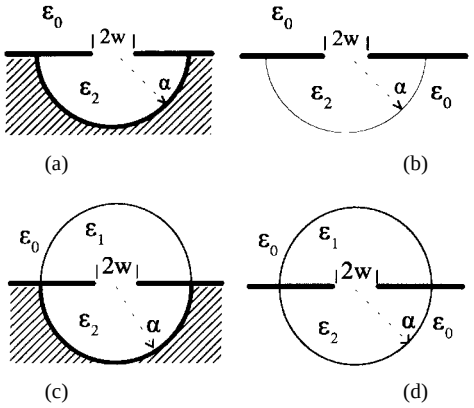

Fig. 3. Practical configurations derivable from the structure of Fig. 1 as special cases.

as well; we note that for these latter problems direct tests are not available. The propagation characteristics of all these guiding structures will be investigated in a future paper.

II. Formulation

We begin with the single-slot structure shown in Fig. 1. The slot of width $2w$ (placed at $y = 0, d-w \le x \le d+w, -\infty < z < \infty$) is covered by two semicircular dielectric cylinders of radii α_1 and α_2 (regions 1 and 2 in general lossy) surrounded by regions 0 and 3, respectively. For simplicity of notation, the cylinders are taken to be coaxial with their common axis displaced from the slot axis by d.

A. Definitions

Assuming an arbitrarily polarized plane wave $(\bar{E}^{\rm inc}, \bar{H}^{\rm inc}) = (\hat{z}E_z^{\rm inc} + \bar{E}_t^{\rm inc}, \hat{z}H_z^{\rm inc} + \bar{H}_t^{\rm inc})$ obliquely incident in the direction of $\bar{k}_0(k_0,\theta_0,\varphi_0) = k_0(\sin\theta_0\cos\varphi_0\hat{x} + \sin\theta_0\sin\varphi_0\hat{y} + \cos\theta_0\hat{z})$ $(k_0 = \omega\sqrt{\varepsilon_0\mu_0})$ let $(E_z^{\rm inc}, H_z^{\rm inc}) = (E_0, H_0)e^{j\bar{k}_0\cdot\bar{r}}$ (the $\exp(j\omega t)$ time-dependence has been supressed).

The field $(\bar{E}^{\rm exc}(\bar{\rho}), \bar{H}^{\rm exc}(\bar{\rho}))e^{j\beta z}$ excited at $\bar{\rho}(\rho,\varphi) \in (1)$ by the incident wave when $w = 0$ (slot absent or short-circuited) will be termed excitation field. Its z components may be expanded as follows:

$$\begin{pmatrix} E_z^{\rm exc}(\bar{\rho}) \\ E_z^{\rm exc}(\bar{\rho}) \end{pmatrix} = 2\sum_{n=0}^{\infty} \epsilon_n J_n(k_{\rm cl}\rho) j^n \times \begin{pmatrix} \sin(n\varphi)\left[a_n^E \sin(n\varphi_0) + j a_n^H \cos(n\varphi_0)\right] \\ \cos(n\varphi)\left[-j b_n^E \sin(n\varphi_0) + b_n^H \cos(n\varphi_0)\right] \end{pmatrix} \tag{1}$$

where $\epsilon_n = 2 - \delta_{n0}$ is Neumann's factor, $k_{\rm cl}^2 = k_1^2 - \beta^2 = \omega^2\varepsilon_1\mu_1 - \beta^2$, $\beta = k_0\cos\theta_0$, and $J_n(\cdot)$ denotes the Bessel function of order n. The expressions of $(a_n^Q, b_n^Q; Q \equiv E, H)$ are given in (A.1).

Let $[\bar{E}^{\rm tot}(\bar{\rho}), \bar{H}^{\rm tot}(\bar{\rho})]e^{j\beta z}$ be the total field at $\bar{\rho}(x,y)$ in the presence of the slot $(w \neq 0)$. Then the field $[\bar{E}^{\rm scat}(\bar{\rho}), \bar{H}^{\rm scat}(\bar{\rho})]e^{j\beta z} = [\bar{E}^{\rm tot}(\bar{\rho}) - \bar{E}^{\rm exc}(\bar{\rho}), \bar{H}^{\rm tot}(\bar{\rho}) - \bar{H}^{\rm exc}(\bar{\rho})]e^{j\beta z}$ will be called scattered field. Define the equivalent surface magnetic current $\bar{M}(x) = \bar{E}^{\rm scat}(x,0) \times \hat{y} = [\hat{x}M_x(x) + \hat{z}M_x(x)]e^{j\beta z}$. Following field equivalence principles, the scattered field for $y > 0$ $(y < 0)$ may be considered as produced by $\bar{M}$ $(-\bar{M})$ acting in the absence of the slot.

Let $[{}^J\bar{E}^s(\bar{\rho},\bar{\rho}'), {}^J\bar{H}^s(\bar{\rho},\bar{\rho}')]e^{-j\beta z}$ and $[{}^M\bar{E}^s(\bar{\rho},\bar{\rho}'), {}^M\bar{H}^s(\bar{\rho},\bar{\rho}')]e^{-j\beta z}$ be the fields excited at $\bar{\rho}(\rho,\varphi) \in (s)$ $(s = 1,2)$ by the unit line-sources $\bar{J}_a = \hat{z}I_a\delta(\bar{\rho} - \bar{\rho}')e^{-j\beta z}$ $(I_a = 1$ A) and $\bar{M}_a = \hat{z}M_a\delta(\bar{\rho} - \bar{\rho}')e^{-j\beta z}$ $(M_a = 1$ V), respectively, impressed at $\bar{\rho}'(\rho',\varphi') \in (s)$ in the absence of the slot $(w = 0)$. Its z components may be expanded as follows:

$$\begin{aligned} &\begin{pmatrix} {}^Q E_z^s \\ {}^Q H_z^s \end{pmatrix} \\ &= -\frac{k_{cs}^2}{4\omega}\begin{pmatrix} I_a\delta_{QJ}\varepsilon_s^{-1}(H_0(k_{cs}R^-) - H_0(k_{cs}R^+)) \\ M_a\delta_{QM}\mu_s^{-1}(H_0(k_{cs}R^-) + H_0(k_{cs}R^+)) \end{pmatrix} \\ &\quad + 2\sum_{n=0}^{\infty}\epsilon_n \begin{pmatrix} A_n^Q \sin(n\varphi)(\delta_{QJ}\sin(n\varphi') + j\delta_{QM}\cos(n\varphi')) \\ B_n^Q \cos(n\varphi)(-j\delta_{QJ}\sin(n\varphi') + \delta_{QM}\cos(n\varphi')) \end{pmatrix} \\ &\quad \times J_n(k_{cs}\rho)J_n(k_{cs}\rho'); \quad Q \equiv J, M \end{aligned} \tag{2}$$

where $\delta_{QP} = 1$, if $Q \equiv P, 0$ otherwise, $R^{\pm} = \sqrt{(x-x')^2 + (y \pm y')^2}$ and $H_n(\cdot)$ is the Hankel function of the second kind and of order n. The expansion constants (A_n^Q, B_n^Q) are identified with $(A_n^Q(s,s), B_n^Q(s,s))$ specified as in (A.2) (for $s = 1$), (A.3) (for $s = 2$ when region 3 is a dielectric), and (A.4) (for $s = 2$ when region 3 is a perfect electric conductor).

B. Formulation of the System of SIE-SIDE

Using the reaction theorem twice in the way outlined in [10] we get

$$\begin{aligned} M_a H_z^{\rm scat}(\bar{\rho}') = {\rm sgn(y')} \int_C \big[&{\rm M_x(x)}\,{}^{\rm M}{\rm H_x^s(x,0;\bar{\rho}')} \\ &+ M_z(x)\,{}^M H_z^s(x,0;\bar{\rho}')\big]\,dx \end{aligned} \tag{3a}$$

$$\begin{aligned} -I_a E_z^{\rm scat}(\bar{\rho}') = {\rm sgn}(y') \int_C \big[&M_x(x)\,{}^J H_x^s(x,0;\bar{\rho}') \\ &+ M_z(x)\,{}^J H_z^s(x,0;\bar{\rho}')\big]\,dx \end{aligned} \tag{3b}$$

where C denotes the x-axis interval $d-w \le x \le d+w$. Note that z has been most naturally eliminated from (3a) and (3b)

as a result of the $\exp(-j\beta z)$ dependence adopted for both $\bar{J}_a$ and $\bar{M}_a$ and the $\exp(j\beta z)$ dependence for $\bar{E}^{\rm scat}, \bar{H}^{\rm scat}$.

Let $(y'=0, x' \in C)$ in (3a). Using the relation $jk_{cs}^2 {}^M H_x^s(\bar{\rho},\bar{\rho}') = \beta\partial[{}^M H_z^s(\bar{\rho},\bar{\rho}')]/\partial x - \omega\varepsilon_s\partial[{}^M E_z^s(\bar{\rho},\bar{\rho}')]/\partial y$ in conjuction with the boundary condition $H_z^{\rm scat}(x',0^+) + H_z^{\rm exc}(x',0^+) = H_z^{\rm scat}(x',0^-)(x' \in C)$ we end up with the SIE

$$\begin{aligned}
&\mathcal{L}\{C; M_z, M_x; x'\} \\
&\quad \equiv \sum_{s=1}^{2}\Bigg\{-k_c^2 L(M_z) - j\beta\frac{d}{dx'}L(M_x) \\
&\qquad + \sum_{n=0}^{\infty}\epsilon_n J_n(k_c x')\Bigg[2B_n^M\int_C M_z(x)J_n(k_c x)\,dx \\
&\qquad - \frac{1}{k_c}\int_C M_x(x)\big[j\beta B_n^M h_n^-(k_c x) \\
&\qquad + \omega\varepsilon A_n^M h_n^+(k_c x)\big]\,dx\Bigg]\Bigg\} \\
&\quad = -H_z^{\rm exc}(x',0)(x' \in C). \qquad (4)
\end{aligned}$$

Here (and throughout the analysis that follows)

$$L(M) = L(M;x') = \frac{1}{2\omega\mu}\int_C M(x)H_0(k_c|x-x'|)\,dx \qquad (5)$$

$$(k_c,\varepsilon,\mu) \equiv (k_{cs},\varepsilon_s,\mu_s) \qquad (6)$$

whereas $h_n^{\pm}$ stand for

$$h_n^{\pm}(k_c x) = J_{n-1}(k_c x) \pm J_{n+1}(k_c x). \qquad (7)$$

The second SIDE of the problem may be constructed as follows: re-express ${}^J H_x^s$ and ${}^M H_x^s$ in (3a) and (3b) in terms of $({}^J E_z^s, {}^J H_z^s)$ and $({}^M E_z^s, {}^M H_z^s)$, respectively, and use the relation $jk_{cs}^2 H_x^{\rm scat}(x',y') = -\beta\partial[H_z^{\rm scat}(x',y')]/\partial x' - \omega\varepsilon_s\partial[E_z^{\rm scat}(x',y')]/\partial y'$; $(x',y') \in (s)$. Set $(y'=0, x' \in C)$ and apply the boundary condition $H_x^{\rm scat}(x',0^+) + H_x^{\rm exc}(x',0^+) = H_x^{\rm scat}(x',0^-)$. Then, after some lengthy algebraic manipulations, we end up with the SIDE

$$\begin{aligned}
&\mathcal{F}(C; M_z, M_x; x') \\
&\quad \equiv \sum_{s=1}^{2}\Bigg\{-j\beta\frac{d}{dx'}L(M_z) - \left[\frac{d^2}{dx'^2}+k^2\right]L(M_x) \\
&\qquad + \frac{1}{k_c}\sum_{n=0}^{\infty}\epsilon_n\Bigg[\big(j\beta B_n^M h_n^-(k_c x') - \omega\varepsilon B_n^J h_n^+(k_c x')\big) \\
&\qquad \cdot \int_C M_z(x)J_n(k_c x)dx \\
&\qquad + \frac{1}{2k_c}\int_C M_x(x)\big[h_n^-(k_c x')\big(\beta^2 B_n^M h_n^-(k_c x) \\
&\qquad - j\omega\varepsilon\beta A_n^M h_n^+(k_c x)\big) + h_n^+(k_c x')\big((\omega\varepsilon)^2 A_n^J h_n^+(k_c x) \\
&\qquad + j\omega\varepsilon\beta B_n^J h_n^-(k_c x)\big)\big]\,dx\Bigg]\Bigg\} \\
&\quad = -H_x^{\rm exc}(x',0) \quad (x' \in C). \qquad (8)
\end{aligned}$$

Here, in addition to (6), $k \equiv k_s$.

C. Solution of the System of (4) and (8)

We set $x = d + wt$, $x' = d + wt'$ $(-1 \le t, t' \le 1)$. In view of the edge conditions, M_z and M_x are most conveniently expanded into series of Chebyshev polynomials

$$\begin{aligned}
M_z[x(t)] &= (1-t^2)^{-1/2}\sum_{N=0}^{\infty} a_N T_N(t) \\
M_x[x(t)] &= (1-t^2)^{1/2}\sum_{N=0}^{\infty} b_N U_N(t) \quad t=(x-d)/w. \qquad (9)
\end{aligned}$$

Substitution from (9) into (4) and (8) and following the discretization procedure outlined in [11]–[12] yields the following linear algebraic system in a_N and b_N

$$\begin{aligned}
&\sum_{N=0}^{\infty}\big[a_N R_{MN}^{zz} + b_N R_{MN}^{zx}\big] = \tilde{c}_M \\
&\sum_{N=0}^{\infty}\big[a_N R_{MN}^{xz} + b_N R_{MN}^{xx}\big] = \tilde{d}_M; \quad M = 0,1,2,\cdots,\infty \qquad (10)
\end{aligned}$$

where

$$\begin{aligned}
R_{MN}^{zz} &= R_{MN}^{zz}(w,d) = w\sum_{s=1}^{2}\Bigg[\frac{-k_{cs}^2}{2\omega\mu_s}A_{MN} \\
&\qquad + 2\sum_{n=0}^{\infty}\epsilon_n B_n^M S_I^s(M,n)S_I^s(N,n)\Bigg] \qquad (11a) \\
R_{MN}^{xz} &= R_{MN}^{xz}(w,d) \\
&= \sum_{s=1}^{2}\Bigg[\frac{-j\beta}{2\omega\mu_s}C_{MN} + \frac{w}{k_{cs}}\sum_{n=0}^{\infty}\epsilon_n\big[j\beta B_n^M \tilde{S}_-^s(M,n) \\
&\qquad - \omega\varepsilon_s B_n^J \tilde{S}_+^s(M,n)\big]S_I^s(N,n)\Bigg] \qquad (11b) \\
R_{MN}^{zx} &= R_{MN}^{zx}(w,d) = -R_{NM}^{xz}(w,d) \qquad (11c) \\
R_{MN}^{xx} &= R_{MN}^{xx}(w,d) \\
&= \sum_{s=1}^{2}\Bigg\{\frac{-1}{2\omega\mu_s w}D_{MN} \\
&\qquad + \frac{w}{2k_{cs}^2}\sum_{n=0}^{\infty}\epsilon_n\big[\beta^2 B_n^M \tilde{S}_-^s(M,n)\tilde{S}_-^s(N,n) \\
&\qquad + (\omega\varepsilon_s)^2 A_n^J \tilde{S}_+^s(M,n)\tilde{S}_+^s(N,n) \\
&\qquad - j\omega\varepsilon_s\beta A_n^M(\tilde{S}_-^s(M,n)\tilde{S}_+^s(N,n) \\
&\qquad + \tilde{S}_+^s(M,n)\tilde{S}_-^s(N,n))\big]\Bigg\} \qquad (11d)
\end{aligned}$$

$$\begin{aligned}
\tilde{c}_M &= \tilde{c}_M(w,d) \\
&= -2\sum_{n=0}^{\infty}\epsilon_n j^n\big(-jb_n^E\sin(n\varphi_0) + b_n^H\cos(n\varphi_0)\big)S_I^1(M,n) \qquad (11e) \\
\tilde{d}_M &= \tilde{d}_M(w,d) \\
&= \frac{-j}{k_{cl}}\sum_{n=0}^{\infty}\epsilon_n j^n\big[\beta\big(-jb_n^E\sin(n\varphi_0) \\
&\qquad + b_n^H\cos(n\varphi_0)\big)\tilde{S}_-^1(M,n) + \omega\varepsilon_1\big(a_n^E\sin(n\varphi_0) \\
&\qquad + ja_n^H\cos(n\varphi_0)\big)\tilde{S}_+^1(M,n)\big]. \qquad (11f)
\end{aligned}$$

In (11)

1) $A_{MN} \equiv A_{MN}(k_{cs}w)$, $C_{MN} \equiv C_{MN}(k_{cs}w)$, and $D_{MN} \equiv D_{MN}(k_s^2, k_{cs}w)$—originating from the singular part of the kernels—assume the analytical, very efficient expressions given by [12, eq. (24), (27), (30)] (see also [11]);
2) S_p^s and $\tilde{S}_\pm^s$ are shorthand symbols for

$$S_p^s(M,n) = S_p^s(M,n;k_{cs}w,k_{cs}d) = \sum_{m=0}^{\infty} \frac{\epsilon_m}{2}[J_{n-m}(k_{cs}d) + (-1)^m J_{n+m}(k_{cs}d)] \times P(M,m;k_{cs}w); \quad P \equiv I,\Lambda \tag{12a}$$

$$\tilde{S}_\pm^s(M,n) = \tilde{S}_\pm^s(M,n;k_{cs}w,k_{cs}d) = S_\Lambda^s(M,n-1) \pm S_\Lambda^s(M,n+1) \tag{12b}$$

where

$$I(p,q;k_{cs}w) = \pi J_{(q+p)/2}(k_{cs}w/2)J_{(q-p)/2}(k_{cs}w/2) \quad \text{if } p+q \text{ is even, 0 otherwise,} \tag{13a}$$

$$\Lambda(p,q;k_{cs}w) = [I(p,q) - I(p+2,q)]/2. \tag{13b}$$

One observes that when $d = 0$ (symmetrically placed fins) $S_p^s(N,n) = P(N,n;k_{cs}w)$ $(P \equiv I,\Lambda)$. In such a case, therefore, (11a)–(11f) involves single exponentially converging series only.

D. Scattered Field

The z components of the scattered field at (ρ,φ) in regions $q = 0$ and $q = 3$ assume the following analytical expressions

$$\begin{pmatrix} E_z^{(q)}(\rho,\varphi) \\ H_z^{(q)}(\rho,\varphi) \end{pmatrix} = \sum_{n=0}^{\infty} \frac{\epsilon_n}{2} H_n(k_{cq}\rho) \begin{pmatrix} j\sin(n\varphi)\,{}_s^J\Gamma(n) \\ \cos(n\varphi)\,{}_s^M\Gamma(n) \end{pmatrix} \tag{14a}$$

where

$${}_s^Q\Gamma(n) = {}_s^Q\Gamma(n;a_N,b_N,w) = w\sum_{N=0}^{\infty}\Big[a_N 4B_n^Q(s,q)S_I^s(N,n) - b_N\frac{2}{k_{cs}}\big(j\beta B_n^Q(s,q)\tilde{S}_-^s(N,n) + \omega\varepsilon_s A_n^Q(s,q)\tilde{S}_+^s(N,n)\big)\Big] \tag{14b}$$

with $s = 1$ (2) if $q = 0$ (3). The transverse components of the scattered field may be evaluated from their expressions in terms of E_z and H_z. Using the large argument expression for the Hankel function $H_n(k_{cq}\rho) \approx \sqrt{2j/(\pi k_{cq}\rho)}\,j^n e^{-jk_{cq}\rho}$ the field expression (14a) ends up with the corresponding far field.

By integrating the Poynting vector on the surfaces of two semicylinders of infinite radius and on the (double-sided) surface of the slot we obtain for the per unit length far-scattered power in the radial direction the following two alternative expressions:

$$P_r = \sum_{q=0,3}\frac{\omega}{2k_{cq}^2}\left[\mu_q\sum_{n=0}^{\infty}\frac{\epsilon_n}{2}\left|{}_s^M\Gamma(n)\right|^2 + \varepsilon_q\sum_{n=1}^{\infty}\left|{}_s^J\Gamma(n)\right|^2\right] = \frac{w}{2}\mathrm{Re}\left\{\sum_{N=0}^{\infty}(a_N\tilde{c}_N^* + b_N\tilde{d}_N^*)\right\} \tag{15}$$

with s defined just after (14b). Equality of results based on the above two expressions has been observed (within 13 significant decimals) in all cases, thus providing a first partial check on the validity of the algorithm.

III. Double-Slotted Configurations

We now consider the double-slot configuration shown in Fig. 2. The two slots are located, respectively, at $C_1 \equiv \{d_1 - w_1 \le x \le d_1 + w_1\}$ and $C_2 \equiv \{d_2 - w_2 \le x \le d_2 + w_2\}$. The common axis of the two semicylinders is taken to be the z axis of the Cartesian system $(O \cdot xyz)$. In connection with this structure the following relations:

$$\sum_{v=1}^{2}\mathcal{L}\{C_v;M_z^{(v)},M_x^{(v)};x'\} = -H_z^{\mathrm{exc}}(x',0)$$
$$\sum_{v=1}^{2}\mathcal{F}\{C_v;M_z^{(v)},M_x^{(v)};x'\} = -H_z^{\mathrm{exc}}(x',0) \quad (x' \in C_1 \cup C_2) \tag{16}$$

can be written with $\mathcal{L},\mathcal{F}$, defined in (4) and (8). Letting successively $x' \in C_1$ and $x' \in C_2$, (16) yield a 4×4 system of coupled SIE-SIDE with unknowns the surface current densities $M_z^{(v)}, M_x^{(v)}$ across the v-th slot $(v = 1,2)$. In analogy with (9) these densities are expanded as follows:

$$M_z^{(v)}[x(t)] = (1-t^2)^{-1/2}\sum_{N=0}^{\infty}a_N^{(v)}T_N(t)$$
$$M_x^{(v)}[x(t)] = (1-t^2)^{+1/2}\sum_{N=0}^{\infty}b_N^{(v)}U_N(t)$$
$$t = (x - d_v)/w_v. \tag{17}$$

Discretization of (16) yields the following linear algebraic system:

$$\sum_{N=0}^{\infty}\left\{\bar{\bar{R}}_{MN}^{(11)}\begin{bmatrix}a_N^{(1)}\\ b_N^{(1)}\end{bmatrix} + w_2\bar{\bar{R}}_{MN}^{(12)}\begin{bmatrix}a_N^{(2)}\\ b_N^{(2)}\end{bmatrix}\right\} = \begin{bmatrix}\tilde{c}_M^{(1)}\\ \tilde{d}_M^{(1)}\end{bmatrix}$$
$$\sum_{N=0}^{\infty}\left\{w_1\bar{\bar{R}}_{MN}^{(21)}\begin{bmatrix}a_N^{(1)}\\ b_N^{(1)}\end{bmatrix} + \bar{\bar{R}}_{MN}^{(22)}\begin{bmatrix}a_N^{(2)}\\ b_N^{(2)}\end{bmatrix}\right\} = \begin{bmatrix}\tilde{c}_M^{(2)}\\ \tilde{d}_M^{(2)}\end{bmatrix} \tag{18}$$

$(M = 0,1,\cdots,\infty)$. For the elements of the 2×2 matrices $\bar{\bar{R}}_{MN}^{(iv)} = \begin{bmatrix}(R_{MN}^{zz})^{(iv)} & (R_{MN}^{zx})^{(iv)}\\ (R_{MN}^{xz})^{(iv)} & (R_{MN}^{xx})^{(iv)}\end{bmatrix}$ $(i = 1,2; v = 1,2)$ we obtain the following analytical expressions.

1) For $i = v$

$$\left(R_{MN}^{uv}\right)^{(ii)} = R_{MN}^{uv}(w_i,d_i) \quad (u,v \equiv z,x; i = 1,2) \tag{19a}$$

with $R_{MN}^{uv}(w_i,d_i)$ given in (11a)–(11d).
2) For $i \neq v$

$$\left(R_{MN}^{zz}\right)^{(iv)} = 2\sum_{s=1}^{2}\left[k_{cs}^2\Xi_{iv}^{II}(0) + \sum_{n=0}^{\infty}\epsilon_n B_n^M\hat{S}_I^i(M,n)\hat{S}_I^v(N,n)\right] \tag{19b}$$

$$\left(R_{MN}^{zx}\right)^{(iv)} = \sum_{s=1}^{2}\Bigg\{ j\beta k_{cs}\left[\Xi_{iv}^{I\Lambda}(-1) - \Xi_{iv}^{I\Lambda}(1)\right] - \frac{1}{k_{cs}}\sum_{n=0}^{\infty}\epsilon_n\Big[j\beta B_n^M \hat{\tilde{S}}_{-}^{v}(N,n) + \omega\varepsilon_s A_n^M \hat{\tilde{S}}_{+}^{v}(N,n)\Big]\hat{S}_I^i(M,n)\Bigg\} \tag{19c}$$

$$\left(R_{MN}^{xz}\right)^{(iv)} = \sum_{s=1}^{2}\Bigg\{ j\beta k_{cs}\left[\Xi_{iv}^{\Lambda I}(-1) - \Xi_{iv}^{\Lambda I}(1)\right] + \frac{1}{k_{cs}}\sum_{n=0}^{\infty}\epsilon_n\Big[j\beta B_n^M \hat{\tilde{S}}_{-}^{i}(M,n) - \omega\varepsilon_s B_n^J \hat{\tilde{S}}_{+}^{i}(M,n)\Big]\hat{S}_I^v(N,n)\Bigg\} \tag{19d}$$

$$\left(R_{MN}^{xx}\right)^{(iv)} = \frac{1}{2}\sum_{s=1}^{2}\Bigg\{ \Big[4k_s^2\Xi_{iv}^{\Lambda\Lambda}(0) + k_{cs}^2\left(\Xi_{iv}^{\Lambda\Lambda}(-2) + \Xi_{iv}^{\Lambda\Lambda}(2) - 2\Xi_{iv}^{\Lambda\Lambda}(0)\right)\Big] + \frac{1}{k_{cs}^2}\sum_{n=0}^{\infty}\epsilon_n\Big[\beta^2 B_n^M \hat{\tilde{S}}_{-}^{i}(M,n)\hat{\tilde{S}}_{-}^{v}(N,n) + (\omega\varepsilon_s)^2 A_n^J \hat{\tilde{S}}_{+}^{i}(M,n)\hat{\tilde{S}}_{+}^{v}(N,n) + j\omega\beta\varepsilon_s B_n^J(\hat{\tilde{S}}_{-}^{i}(M,n)\hat{\tilde{S}}_{+}^{v}(N,n) + \hat{\tilde{S}}_{+}^{i}(M,n)\hat{\tilde{S}}_{-}^{v}(N,n))\Big]\Bigg\} \tag{19e}$$

where

$$\left(A_n^J, B_n^J, A_n^M, B_n^M\right) \equiv \left(A_n^J(s,s)B_n^J(s,s), A_n^M(s,s), B_n^M(s,s)\right)$$

$$\begin{aligned}\Xi_{iv}^{PQ}(\ell) &\equiv \Xi_{iv}^{PQ}(M,N;\ell) \\ &= \frac{-1}{8\omega\mu_s}\sum_{n=0}^{\infty}\epsilon_n[\delta_{i1}(-1)^n + \delta_{i2}]H_n(k_{cs}(d_1-d_2)) \\ &\quad\times\sum_{n=0}^{\infty}\epsilon_m[P(M,n+\ell+m;k_{cs}w_i) \\ &\quad+(-1)^m[P(M,n+\ell-m;k_{cs}w_i)] \\ &\quad\times Q(N,m;k_{cs}w_v); \quad P,Q\equiv I,\Lambda\end{aligned} \tag{20a}$$

$$\begin{aligned}\hat{S}_P^i(M,n) &= S_P^s(M,n;k_{cs}w_i,k_{cs}d_i) \\ \hat{\tilde{S}}_{\pm}^i(M,n) &= \tilde{S}_{\pm}^s(M,n;k_{cs}w_i,k_{cs}d_i).\end{aligned} \tag{20b}$$

The constant terms in (18) are given by

$$\tilde{c}_M^{(i)} = \tilde{c}_M(w_i,d_i), \quad \tilde{d}_M^{(i)} = \tilde{d}_M(w_i,d_i) \tag{21}$$

with $\tilde{c}_M(w_i,d_i), \tilde{d}_M(w_i,d_i)$ defined in (11e) and (11f).

The per unit length far scattered power in the radial direction is given by the following two alternative expressions:

$$\begin{aligned}P_r &= \sum_{q=0,3}\frac{\omega}{2k_{cq}^2}\left[\mu_q\sum_{n=1}^{\infty}\frac{\epsilon_n}{2}\left|\sum_{v=1}^{2}{}_s^M\Gamma^{(v)}(n)\right|^2 + \varepsilon_q\sum_{n=1}^{\infty}\left|\sum_{v=1}^{2}{}_s^J\Gamma^{(v)}(n)\right|^2\right] \\ &= \sum_{v=1}^{2}\frac{w_v}{2}\mathrm{Re}\left\{\sum_{N=0}^{\infty}\left(a_N^{(v)}\tilde{c}_N^{(v)^*} + b_N^{(v)}\tilde{d}_N^{(v)^*}\right)\right\}\end{aligned} \tag{22}$$

with s defined just after (14b) and ${}_s^Q\Gamma^{(v)}(n) = {}_s^Q\Gamma^{(v)}(n; a_N^{(v)}, b_N^{(v)}, w_v)$.

Equality of results based on the above two expressions for P_r in (22) has been observed (within 13 significant decimals) in all cases that have been worked out, thus providing an initial check of the validity of the algorithm.

IV. Numerical Results and Discussion

To validate our algorithms, internal as well as external tests have been carried out as follows: 1) the energy conservation principle (Poynting theorem)—as tested by separate evaluation and comparison of the two sides of (15) for the single slot and (22) for the double one—was verified to within the round off errors (at least 13 decimals) in all cases and 2) extensive comparisons of RCS and near- and far-field pattern with available results from [1]–[9] have been carried out as discussed below; once more the agreement was excellent.

For $E_0 = \sqrt{\mu_0/\varepsilon_0}H_0 = \sin\theta_0, \varphi_0 = 45°$ and for several values of θ_0, Fig. 4—corresponding to the structure of Fig. 1—shows the equivalent surface magnetic currents $|M_z[(x-d)/w]|$ and $|M_x[(x-d)/w]|$ across a slot placed between two lossy semicylinders surrounded by air.

For the structure of Fig. 3(a) and (b) and for several values of θ_0, Figs. 5 and 6 show normalized total scattering RCS $\sigma/(2w)$ (where $\sigma = 2Z_0\sin^2\theta_0 P_r/(E_0^2 + Z_0^2H_0^2)$) against φ_0 and against $\varepsilon_r = \varepsilon_2/\varepsilon_0$ in the cases of H-polarized\$E$-polarized plane waves. The curves for $\theta_0 = 90°$ (normal incidence) are indistinguishable from those in [1, fig. 4(b)], [1, fig. 8(a)], pointing to the excellent agreement with available results in this special case.

For the sake of comparison with [2] and [3], we exhibit (in Fig. 7) the quantities $P_e = \sqrt{\pi k_{c0}\rho/2}|E_z^{\mathrm{tot}}(\rho,\varphi) - E_z^{\mathrm{inc}}(\rho,\varphi)|$ and $P_h = \sqrt{\pi k_{c0}\rho/2}|H_z^{\mathrm{tot}}(\rho,\varphi) - H_z^{\mathrm{inc}}(\rho,\varphi)|$ versus $k_0\alpha$ for the structure of Fig. 3(c), for $\varphi = \varphi_0 = 90°$ and for several values of θ_0 in the case of E- [Fig. 7(a)] or H-polarization [Fig. 7(b)]. The curves $\theta_0 = 90°$ are again indistinguishable from those in [2, Fig. 4] and [3, Fig. 3(b)]. [We also reproduced all curves of [2, Figs. 3–6], [3, Figs. 2(a), 3(a), 3(b)], [5, Figs. 2–4], and [6, Figs. 2–5] (not shown)].

For the sake of comparison with the results of [4] in Fig. 8 we show the near-field pattern $E_z^{\mathrm{tot}}(\alpha,\varphi)$ versus φ in the case of E-polarization for the structure of Fig. 3(c), for

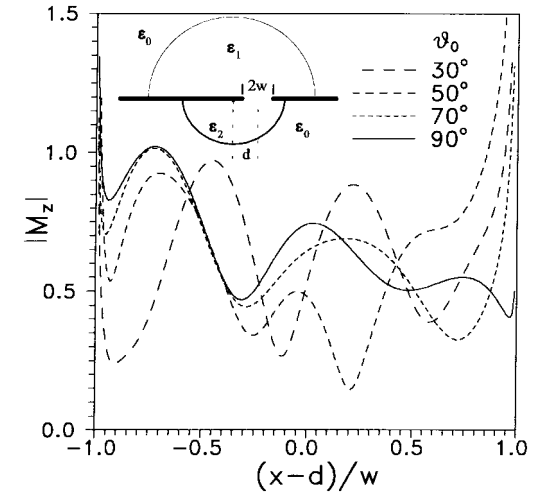

(a)

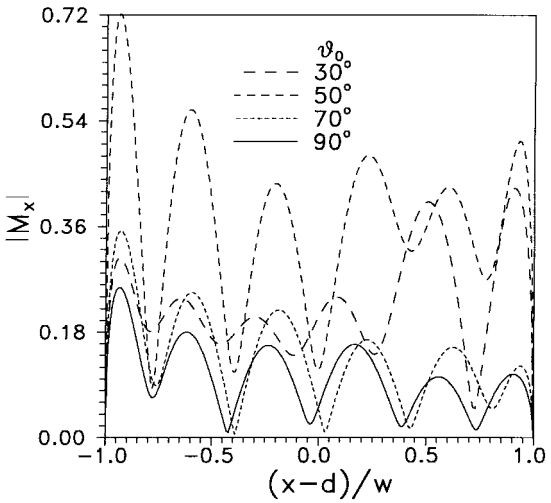

(b)

Fig. 4. Surface magnetic current distribution for $\varphi_0 = 45°$ and for several values of θ_0 (structure of Fig. 1, $2w = \lambda_0$, $d = 0.25\lambda_0$, $\alpha_1 = 2\lambda_0$, $\alpha_2 = \lambda_0$, $\varepsilon_1 = 3(1 - j30)\varepsilon_0$, $\varepsilon_2 = 5(1 - j30)\varepsilon_0$, $\varepsilon_3 = \varepsilon_0$, $E_0 = Z_0 H_0 = \sin\theta_0$).

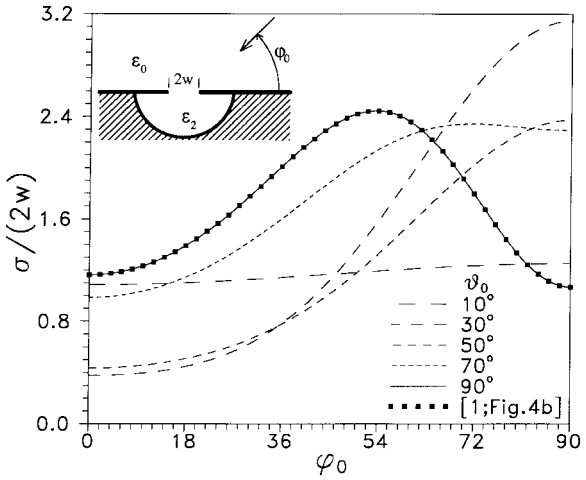

Fig. 5. Normalized total scattering RCS of the structure of Fig. 3(a) versus φ_0 for $2w = \lambda_0$, $d = 0$, $\alpha = \lambda_0$, $\varepsilon_2 = \varepsilon_0$, $E_0 = 0$, $H_0 = 1$, and for several values of θ_0.

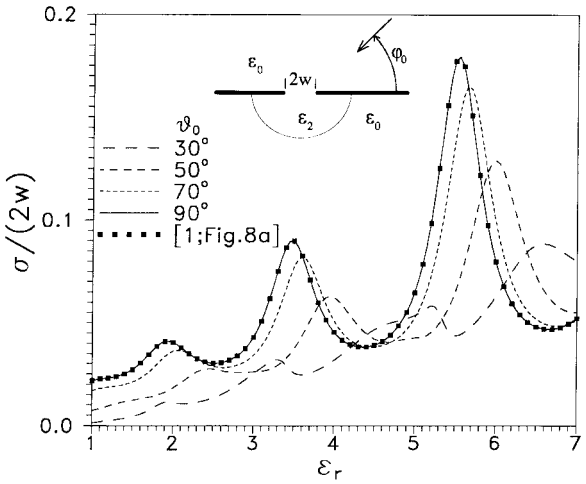

Fig. 6. Normalized total scattering RCS for the structure of Fig. 3(b) versus ε_r for $\varphi_0 = 90°$ and for several values of θ_0 in case $2w = 0.1\lambda_0$, $d = 0$, $\alpha = \lambda_0$, $E_0 = 1$, $H_0 = 0$.

$\varphi_0 = 90°$ and for several values of θ_0. The curves $\theta_0 = 90°$ are indistinguishable from the previous ones in [4, Fig. 8(b)]. (The same was observed when we reproduced all curves of [4, Fig. 9(b)]).

Comparing further with the results in [7] and [8], we show in Fig. 9, corresponding to Fig. 3(d), $\varphi_0 = 90°$ and variable θ_0, the transmission coefficients $t_E = (2k_{c0}\alpha)^{-1}\sum_{n=0}^{\infty}|{}_2^J\Gamma(n)|^2$ and $t_H = (2k_{c0}\alpha)^{-1}\sum_{n=0}^{\infty}|{}_2^M\Gamma(n)|^2$ versus $k_0\alpha$; ${}_2^J\Gamma(n)$, ${}_2^M\Gamma(n)$ are defined in (14b). The curves $\theta_0 = 90°$ are indistinguishable from those in [8, Figs. 5(b), 5(a)]. We also reproduced all curves of [7, Figs. 3–6], [8, Figs. 5, 6], and the curves for the unloaded slit of [8, Figs. 7, 8].

As noted in the introduction, dielectrically loaded slots may be designed to achieve RCS reduction and control. These possibilities are illustrated in Figs. 10 and 11 where σ/λ_0 is shown versus φ_0. In Fig. 10, corresponding to the structure of Fig. 1, one may observe the strong effect on RCS when both φ_0 and ε_1, ε_2 are changed. Reductions of about 6–20 dB from the unloaded case $\varepsilon_1 = \varepsilon_2 = \varepsilon_0$ are possible over the whole range of the angle of incidence φ_0. In Fig. 11, related to the structure of Fig. 2, a considerable reduction of σ/λ_0 is indicated by properly selecting φ_0 and/or ε_1, ε_2. For instance the choice $\varepsilon_1 = \varepsilon_2 = 17\varepsilon_0$ and $\varphi_0 \approx 90°$ reduces the RCS by about 20 dB from the unloaded case.

Convergence of the algorithm is illustrated in Table I where values of $|M_z(x = 0)|, |M_x(x = 0)|, \sigma/\lambda_0$ are shown for several truncation sizes N_r, the number of basis functions used in (9). These values correspond to the structure of Fig. 1 when $2w = \lambda_0$, $d = 0$, $\alpha_1 = \alpha_2 = \lambda_0$, $\varepsilon_1 = \varepsilon_2 = 2\varepsilon_0$, $\varepsilon_3 = \varepsilon_0$, $\theta_0 = \varphi_0 = 45°$, $E_0 = Z_0 H_0 = 1$. Obviously, the convergence is very rapid and stable; $N_r = 14$, for instance, suffices to evaluate the current densities within seven significant decimals. For the far-field quantity σ/λ_0, this same accuracy is achieved for much smaller values of N_r, as expected.

As an indication of the efficiency of our algorithms in Table II, we present values of the transmission coefficient of an unloaded slot for several $k\alpha$ values ($k = k_1 = k_2 = k_3 = k_0$),

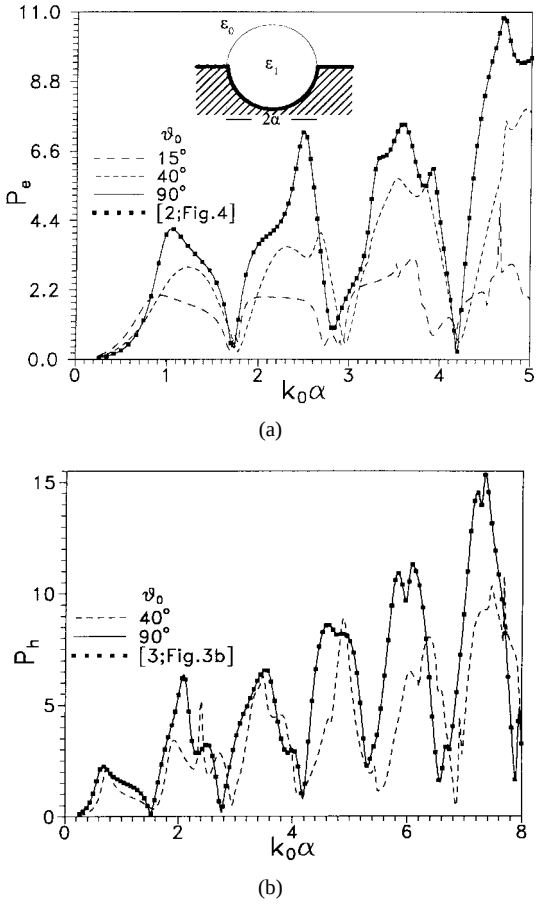

Fig. 7. Far field amplitude versus $k_0\alpha$ for the structure of Fig. 3(c) for $\varphi_0 = 90°$ and for several values of θ_0 in case $\varepsilon_1 = \varepsilon_2 = 3\varepsilon_0$, $\alpha = w$, $d = 0$. (a) $E_0 = 1, H_0 = 0$. (b) $E_0 = 0, H_0 = 1$.

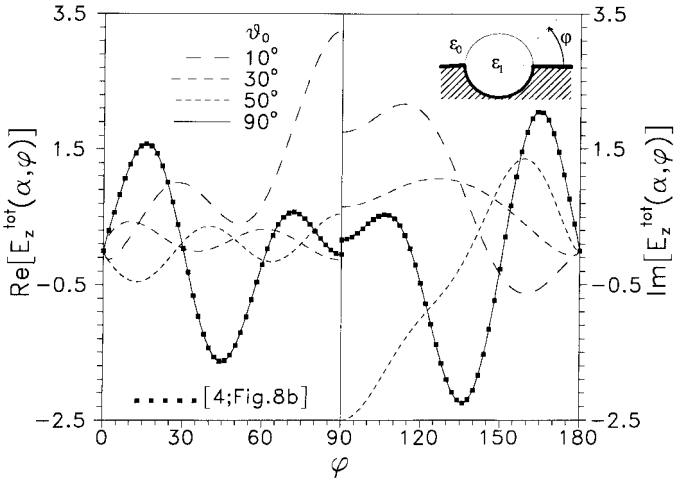

Fig. 8. Near field pattern of the structure of Fig. 3(c) in case $E_0 = 1$, $H_0 = 0$, $\varepsilon_1 = \varepsilon_2 = 2.5\varepsilon_0$, $\alpha = w = \lambda_0$, $d = 0$, $\varphi_0 = 90°$, for several values of θ_0.

in case of normally incident $(\theta_0 = \varphi_0 = 90°)$, E-polarized $(E_0 = 1, H_0 = 0)$ plane waves. For this special case, exact results are available in [9] (based on separation of variables techniques using Mathieu functions). As seen, a value of N_r less than nine ensures a very high accuracy (of at least five significant decimals) in all cases.

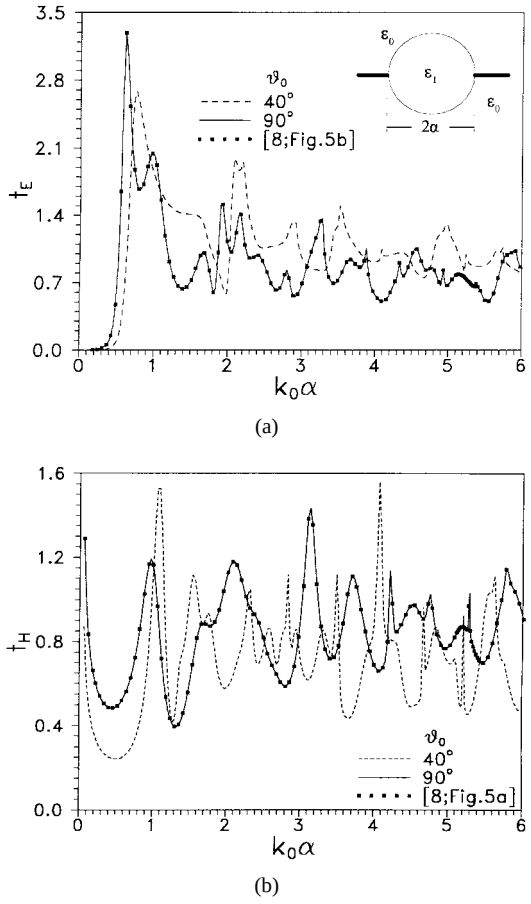

Fig. 9. Transmission coefficient versus $k_0\alpha$ for the structure of Fig. 3(d) for $\varphi_0 = 90°$ and for several values of θ_0 in case $\varepsilon_1 = \varepsilon_2 = 5\varepsilon_0$, $\alpha = w$, $d = 0$. (a) $E_0 = 1, H_0 = 0$ (E-polarization). (b) $E_0 = 0, H_0 = 1$ (H-polarization).

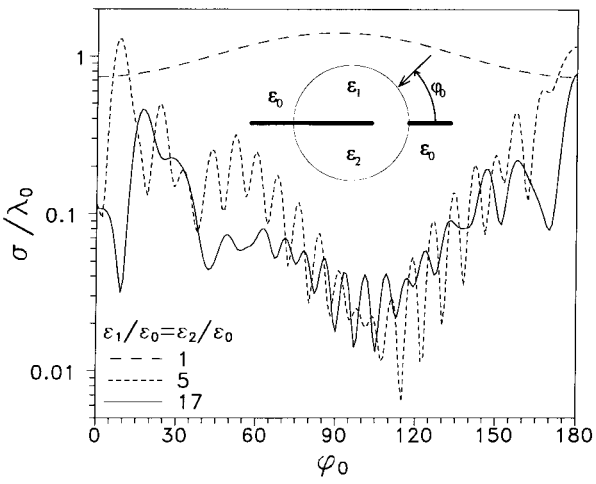

Fig. 10. Total scattering RCS for the structure of Fig. 1 versus φ_0 in case $E_0 = H_0 = 1$, $\varepsilon_1 = \varepsilon_2$, $\varepsilon_3 = \varepsilon_0$, $\theta_0 = 45°$, $2w = \lambda_0$, $d = 4.5\lambda_0$, $\alpha_1 = \alpha_2 = 5\lambda_0$.

V. Conclusion

An efficient analysis based on direct SIE-SIDE methods has been presented for the diffraction problems connected with slots loaded by dielectric semicylinders in the most general case of oblique incidence of arbitrarily polarized plane

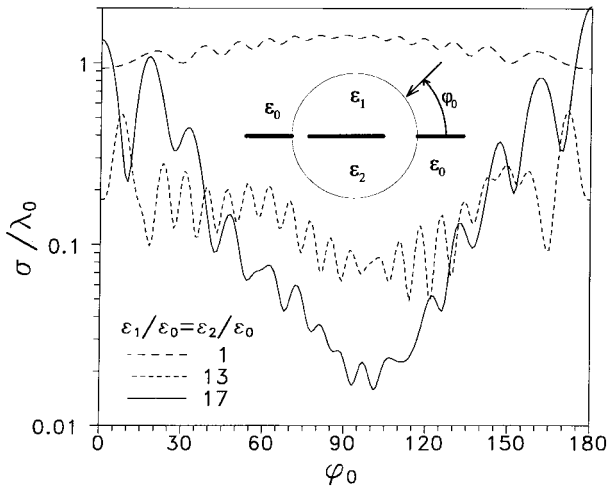

Fig. 11. Total scattering RCS for the structure of Fig. 2 versus φ_0 in case $E_0 = H_0 = 1$, $\varepsilon_1 - \varepsilon_2$, $\varepsilon_3 = \varepsilon_0$, $\theta_0 = 45°$, $2w_1 = 0.6\lambda_0$, $d_1 = 4.7\lambda_0$, $2w_2 = 0.4\lambda_0$, $d_2 = -4.8\lambda_0$, $\alpha_1 = \alpha_2 = 5\lambda_0$.

TABLE I
CONVERGENCE OF THE ALGORITHM

N_r	$\lvert M_z(x=0)\rvert$	$\lvert M_x(x=0)\rvert$	σ/λ_0
6	0.457963442	0.897696230	1.475153307
8	0.463237152	0.915710969	1.475390516
11	0.463909651	0.916578018	1.475390805
14	0.463911643	0.916568586	1.475390805
16	0.463911694	0.916568596	1.475390805

TABLE II
TRANSMISSION COEFFICIENT OF AN UNLOADED SLIT

	Present theory ($N_r = 9$)	Exact values [9]
$k\alpha$	t_0	
0.2	0.00262388	0.00262
0.8	0.26058989	0.26059
1.0	0.54540195	0.54540
1.2	0.87692599	0.87693
1.8	1.22128800	1.22129
2.0	1.18425767	1.18426
2.4	1.08650905	1.08650
3.0	0.97201840	0.97202
3.4	0.92824095	0.92824
4.0	0.94243633	0.94244

waves. Our numerical results reveal that RCS reduction may be achieved by properly selecting several parameters (such as the dielectric constants, the eccentricity, and/or the angle of incidence). To validate the numerical codes that have been developed, internal and external tests have been applied extensively. These same algorithms may be readily used for treating the corresponding homogeneous problems describing propagation in these same structures as will be shown in a future paper.

APPENDIX

Let us define

$$\bar{\bar{U}}_i^p(\beta,\alpha) = k_{ci}^{-1}\begin{pmatrix} \frac{\beta n}{k_{ci}\alpha}h_n^p(k_{ci}\alpha) & -j\omega\mu_i\left(h_n^p(k_{ci}\alpha)\right)' \\ j\omega\varepsilon_i\left(h_n^p(k_{ci}\alpha)\right)' & \frac{\beta n}{k_{ci}\alpha}h_n^p(k_{ci}\alpha)\end{pmatrix} \quad (i=0,1,2,3;\ p=0,1,2,3)$$

with $h_n^p(\cdot) = J_n(\cdot)$ (if $p = 1$ or $p = 2$); $H_n(\cdot)$ (if $p = 0$ or $p = 3$) (the prime denotes the derivative with respect to argument).

Evaluation of $\bar{x} = (a_n^Q, b_n^Q)^T (Q \equiv E, H)$*:*

$$\bar{x} = \left[J_n(k_{c1}\alpha_1)\bar{\bar{U}}_0^0(\beta,\alpha_1) - H_n(k_{c0}\alpha_1)\bar{\bar{U}}_1^1(\beta,\alpha_1)\right]^{-1} \cdot \left[J_n(k_{c0}\alpha_1)\bar{\bar{U}}_0^0(\beta,\alpha_1) - H_n(k_{c0}\alpha_1)\bar{\bar{U}}_0^1(\beta,\alpha_1)\right] \cdot \begin{pmatrix}\delta_{QE}E_0 \\ \delta_{QH}H_0\end{pmatrix}. \quad \text{(A.1)}$$

Evaluation of $\bar{x}_0 = (A_n^Q(0,s), B_n^Q(0,s))^T, \bar{x}_1 = (A_n^Q(1,s), B_n^Q(1,s))^T; (s = 0,1), (Q \equiv J, M)$*:* $\bar{x}_0$ and $\bar{x}_1$ are determined from the 4×4 linear system

$$H_n(k_{c0}\alpha_1)\bar{x}_0 - J_n(k_{c1}\alpha_1)\bar{x}_1 = \delta_{s0}J_n(k_{cs}\alpha_1)\bar{d} - \delta_{s1}H_n(k_{cs}\alpha_1)\bar{d}, \quad \text{(A.2a)}$$

$$\bar{\bar{U}}_0^0(-\beta,\alpha_1)\bar{x}_0 - \bar{\bar{U}}_1^1(-\beta,\alpha_1)\bar{x}_1 = \delta_{s0}\bar{\bar{U}}_s^1(-\beta,\alpha_1)\bar{d} - \delta_{s1}\bar{\bar{U}}_s^0(-\beta,\alpha_1)\bar{d} \quad \text{(A.2b)}$$

where $\bar{d} = \frac{k_{cs}^2}{4\omega}(I_a\delta_{QJ}\varepsilon_s^{-1}, M_a\delta_{QM}\mu_s^{-1})^T$.

Evaluation of $(A_n^Q(3,s), B_n^Q(3,s)), (A_n^Q(2,s), B_n^Q(2,s)); (s = 2,3), (Q \equiv J, M)$*:*

1) When region 3 is a dielectric $\bar{x}_3 = (A_n^Q(3,s), B_n^Q(3,s))^T$ and $\bar{x}_2 = (A_n^Q(2,s), B_n^Q(2,s))^T$ are determined from the 4×4 linear system

$$H_n(k_{c3}\alpha_2)\bar{x}_3 - J_n(k_{c2}\alpha_2)\bar{x}_2 = \delta_{s3}J_n(k_{cs}\alpha_2)\bar{d} - \delta_{s2}H_n(k_{cs}\alpha_2)\bar{d} \quad \text{(A.3a)}$$

$$\bar{\bar{U}}_3^3(-\beta,\alpha_2)\bar{x}_3 - \bar{\bar{U}}_2^2(-(\beta,\alpha_2)\bar{x}_2 = \delta_{s3}\bar{\bar{U}}_s^2(-\beta,\alpha_2)\bar{d} - \delta_{s2}\bar{\bar{U}}_s^3(-\beta,\alpha_2)\bar{d}. \quad \text{(A.3b)}$$

2) When region 3 is a perfect electric conductor then

$$A_n^Q(2,2) = \delta_{QJ}\frac{I_a k_{c2}^2}{4\omega\varepsilon_2}\frac{H_n(k_{c2}\alpha_2)}{J_n(k_{c2}\alpha_2)}$$
$$B_n^Q(2,2) = \delta_{QM}\frac{M_a k_{c2}^2}{4\omega\mu_2}\frac{H_n'(k_{c2}\alpha_2)}{J_n'(k_{c2}\alpha_2)}. \quad \text{(A.4)}$$

REFERENCES

[1] J. L. Tsalamengas, "TE/TM scattering by a slot on a ground plane and in the presence of a semi-cylindrical load," *J. Electron. Waves Applicat.*, vol. 8, no. 5, pp. 613–646, 1994.

[2] T. J. Park, H. J. Eom, W.-M. Boerner, and Y. Yamaguchi, "TM scattering from a dielectric-loaded semi-circular trough in a conducting plane," *IEICE Trans. Commun.*, vol. E75-B, no. 2, pp. 87–91, Feb. 1992.

[3] T. J. Park, H. J. Eom, Y. Yamaguchi, W.-M. Boerner, and S. Kozaki, "TE plane wave scattering from a dielectric-loaded semi-circular trough in a conducting plane," *J. Electron. Waves Applicat.*, vol. 7, no. 2, pp. 235–245, 1993.

[4] M. A. Kolbehdari, H. A. Auda, and A. Z. Elsherbeni, "Scattering from a dielectric cylinder partially embedded in a perfectly conducting ground plane," *J. Electron. Waves Applicat.*, vol. 3, no. 6, pp. 531–554, 1989.

[5] M. K. Hinders and A. D. Yaghjian, "Dual-series solution to scattering from a semicircular channel in a ground plane," *IEEE Microwave Guided Wave Lett.*, vol. 1, pp. 239–242, Sept. 1991.

[6] B. K. Sachdeva and R. A. Hurd, "Scattering by a dielectric-loaded trough in a conducting plane," *J. Appl. Phys.*, vol. 48, no. 4, pp. 1473–1476, Apr. 1977.

[7] R. A. Hurd and B. K. Sachdeva, "Scattering by a dielectric-loaded slit in a conducting plane," *Radio Sci.*, vol. 10, no. 5, pp. 565–572, May 1975.

[8] A. Z. Elsherbeni and H. A. Auda, "Electromagnetic diffraction by two perfectly conducting wedges with dented edges loaded with a dielectric cylinder," *Proc. Inst. Elect. Eng.*, vol. 136, pt. H, no. 3, pp. 225–234, June 1989.

[9] S. Skavlem, "On the diffraction of scalar plane waves by a slit of infinite length," *Arch. Math. Naturvidensk.*, vol. 51, pp. 61–80, 1952.

[10] J. L. Tsalamengas, I. O. Vardiambasis, and J. G. Fikioris, "TE and TM modes in circularly shielded slot waveguides," *IEEE Trans. Microwave Theory Tech.*, vol. 41, pp. 966–973, June/July 1993.

[11] J. L. Tsalamengas and J. G. Fikioris, "Efficient solutions for scattering from strips and slots in the presence of a dielectric half-space: Extension to wide scatterers—Part I: Theory," *J. Appl. Phys.*, vol. 70, no. 3, pp. 1121–1131, Aug. 1991.

[12] J. L. Tsalamengas, "Direct singular integral equation methods in scattering and propagation in strip or slot loaded structures," *IEEE Trans. Antennas Propagat.*, to be published.

Ioannis O. Vardiambasis was born in Athens, Greece, on August 27, 1968. He received the Dipl. and Ph.D. degrees in electrical engineering from the National Technical University of Athens, Greece, in 1991 and 1996, respectively.

In February 1998 he joined the Department of Electronics and Computer Engineering of the Technical University of Crete. His research interests include wave propagation and antennas, radiation and scattering, and applied mathematics.

John L. Tsalamengas (M'87), for a photograph and biography, see p. 555 of the May 1993 issue of this TRANSACTIONS.

John G. Fikioris, for photograph and biography, see p. 555 of the May 1993 issue of this TRANSACTIONS.